JACS
JOURNAL OF THE AMERICAN CHEMICAL SOCIETY
Article
pubs.acs.org/JACS

Catalytic Adaptive Recognition of Thiol (SH) and Selenol (SeH) Groups Toward Synthesis of Functionalized Vinyl Monomers

Valentine P. Ananikov,*[,†] Nikolay V. Orlov,[†] Sergey S. Zalesskiy,[†] Irina P. Beletskaya,[‡] Victor N. Khrustalev,[§] Keiji Morokuma,[∥] and Djamaladdin G. Musaev*[,∥]

[†]Zelinsky Institute of Organic Chemistry, Russian Academy of Sciences, Leninsky Prospect 47, Moscow, 119991, Russia

[‡]Lomonosov Moscow State University, Chemistry Department, Vorob'evy gory, Moscow, 119899, Russia

[§]Nesmeyanov Institute of Organoelement Compounds, Russian Academy of Sciences, Moscow, Russia

[∥]Cherry L. Emerson Center for Scientific Computation and Department of Chemistry, Emory University, Atlanta, Georgia 30322, United States

Supporting Information

ABSTRACT: An unprecedented sustainable procedure was developed to produce functionalized vinyl monomers $H_2C{=}C(R)(FG)$ starting from a mixture of sulfur and selenium compounds as a functional group donor (FG = S or Se). The reaction serves as a model for efficient utilization of natural resources of sulfur feedstock in oil and technological sources of sulfur/selenium. The catalytic system is reported with amazing ability to recognize SH/SeH groups in the mixture and selectively incorporate them into valuable organic products via wastes-free atom-economic reaction with alkynes ($HC{\equiv}CR$). Formation of catalyst active site and the mechanism of the catalytic reaction were revealed by joint experimental and theoretical study. The difference in reactivity of μ_1- and μ_2-type chalcogen atoms attached to the metal was established and was shown to play the key role in the action of palladium catalyst. An approach to solve a challenging problem of dynamically changed reaction mixture was demonstrated using adaptive tuning of the catalyst. The origins of the adaptive tuning effect were investigated at molecular level and were found to be governed by the nature of metal−chalcogen bond.

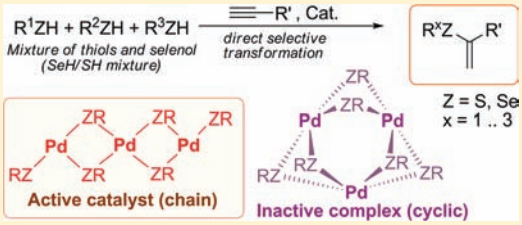

1. INTRODUCTION

The capture, selective recognition and use of thiols, selenols, and their derivatives in organic synthesis are monumental scientific challenges with huge environmental and economical advantages. These vital problems continue to be a focus of scientific and technological communities. Indeed, organosulfur compounds are the most abundant functionalized hydrocarbons available in nature and present as contaminants in crude oil. For environmental protection (to reduce critical SO_2 emissions) and for cost-efficient industrial applications (sulfur species are dangerous poisons of metal catalysts) sulfur removal from crude oil must be performed prior to manufacturing any gasoline, petrol, kerosene, or fuel products. Currently, the petroleum refinery industry uses the rigorously developed industrial hydrodesulfurization process for capture and removal of a mixture of sulfur species from crude oil. This process converts thiols to hydrogen sulfide, which is subsequently transformed to elemental sulfur (Scheme 1).[1−4] To highlight the scale, as large as 68,000,000 t of sulfur were produced worldwide in 2010 with the vast majority coming from hydrocarbon processing plants.[5]

Elemental sulfur serves as a starting reagent for organic synthesis through preparation of single thiols and their subsequent transformation to organic products (Scheme 1). However, such an overall process is highly inefficient (from the point of view of organic synthesis), possesses high energy consumption, and generates a considerable amount of wastes. A sustainable alternative of this multistep and inefficient (energetically and environmentally) process is the direct use of the desired thiols from the crude oil in organic synthesis. Although the idea is well appreciated, its practical realization requires solving several challenging tasks including the separation of individual (desirable for the given organic synthesis) thiols from a mixture of aromatic and aliphatic thiols, sulfides, disulfides, thiophenes, etc. that exist in crude oil.

The selective recognition, capture, and transformation of selenium analogues of thiols (i.e., selenols RSeH and their derivatives) are another challenging task for the environment. Indeed, in spite of a much lower content of selenols RSeH and their derivatives, the handling of these species requires considerable care due to their highly toxic properties and dangerous influence on the environment. Material science applications and microelectronics actively utilize various selenium and sulfur compounds (RZH), thus driving selective capture and removal of chalcogen derivatives in RSeH/RSH mixtures is of the utmost importance.

Received: November 14, 2011
Published: April 4, 2012

   dx.doi.org/10.1021/ja210596w | J. Am. Chem. Soc. 2012, 134, 6637−6649

Scheme 1. Hydrodesulfurization (HDS) of Thiols in Crude Oil, Preparation of Elemental Sulfur, Conversion to a Single Thiol, and Utilization in Organic Synthesis

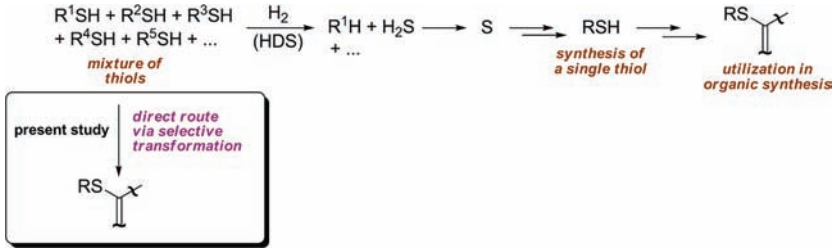

Scheme 2. Direct Involvement of Thiols and Selenols in Organic Synthesis via Addition to Alkynes

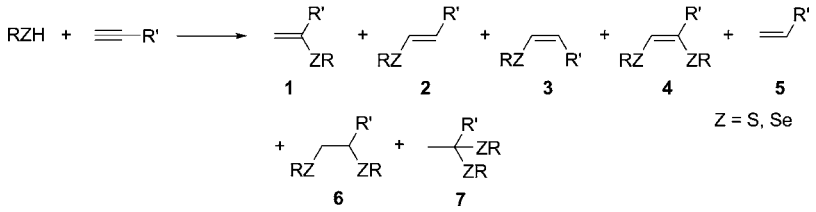

Consequently, the goal of our research is to develop a catalyst for selective recognition and capture of the RZH derivatives (Z = S or Se) and their use as reagents for the preparation of important organic products. For this purpose we have chosen the addition of RZH (Z = S and Se) to the triple bond of acetylenic hydrocarbons (Scheme 2).[6] This addition reaction has a Green Chemistry advantage, as it is 100% atom efficient and does not produce wastes.[7,8] It is important to mention that simple metal salts, particularly $Pd(OAc)_2$, can be used as catalyst precursors to render the catalytic transformation in a selective manner.[9] The proposed reaction utilizes easily available acetylenes as starting material and leads to very useful functionalized vinyl derivatives. Among the possible products **1**–**7**, compound **1** is of substantial interest as a functionalized monomer with significant opportunities as a reagent in organic synthesis, including material and polymer sciences.[10−13] Important to note is that compound **1** is virtually nontoxic or significantly less toxic compared to RZH (Z = S and Se) species, and it does not have an awful odor typical for RSeH and RSH species. This product is not sensitive to air in contrast to RSeH (rapidly oxidized on contact with air) and RSH (slowly oxidized and reacts on air to generate free radicals). Thus, compound **1** is much easier to store and handle and it provides excellent opportunities for industry and organic chemistry.

The transition-metal-catalyzed atom-economic carbon−heteroatom bond formation via the addition reaction to acetylenic hydrocarbons has been the subject of recent studies.[6] Several homogeneous and heterogeneous catalytic systems were investigated for accomplishing the addition of thiols and selenols to multiple carbon−carbon bonds.[6,9,14] It was shown that the metal-catalyzed procedure led to the formation of Markovnikov-type product **1**, while a mixture of anti-Markovnikov derivatives **2** and **3** was formed in the reaction without a metal catalyst. Formation of byproduct **4** from the alkyne and two molecules of thiols was accompanied by evolution of molecular hydrogen, and in situ hydrogenation led to byproduct **5** (Scheme 2).[15,16] Compounds **6** and **7** also can be readily formed after reaction of the second molecule of RZH with alkenes **1**–**3**.[17] Overall, several side reactions leading to byproducts **2**–**7** may take place in the studied system. Thus, achievement of high selectivity in the addition reaction (i.e., exclusive formation of **1**) is a challenging task by itself beyond selective capture of RSH/RSeH from the mixture.

In the present contribution we report a breakthrough heterogeneous Pd-based catalytic system with unprecedented ability for selective synthesis of product **1** starting with a mixture of reagents, RSH/RSeH, and acetylenic hydrocarbons. Importantly, two key factors, (i) selective capture of a reagent from the mixture and (ii) highly selective transformation of each reagent to vinyl monomer **1**, were achieved within a single catalyst. We have developed a procedure that shows high efficiency and selectivity toward RSH and RSeH groups and tolerance to oxygen species and water (Z = O), which may be present in the initial reagents. Furthermore, for practical purposes, the fundamental principles governing these reactions that are vital for designing more efficient catalytic processes were elaborated (experimentally and computationally) by investigating the mechanisms and controlling factors of the reaction of RZH (chalcogen derivatives, where Z = S and Se) with alkynes catalyzed by the newly designed Pd-based catalyst (Scheme 2).

2. RESULTS AND DISCUSSION

2.1. Catalytic Addition Reaction in Multicomponent Mixtures. Addition of catalytic amounts of $Pd(OAc)_2$ as a catalyst precursor to a mixture of chalcogen reagents RZH (Z = S and Se) and acetylenic hydrocarbons generates an active catalyst, which promotes the formation of product **1**. NMR monitoring of the three-component mixture containing phenylselenol, benzenethiol as aromatic thiol, and cyclohexyl thiol as aliphatic thiol (PhSeH/PhSH/CySH = 1:1:1) and 2-methyl-3-butyn-2-ol (3 equiv) as alkyne has revealed outstanding selectivity. At the beginning, the reaction proceeds *exclusively* as addition of PhSeH to the alkyne leading to product **1a** (Figure 1a). None of other components of the mixture (i.e., PhSH and CySH) were involved in the addition reaction until complete utilization of PhSeH (Figure 1b). Furthermore, compound **1a** was the only product formed in the reaction without any other byproduct **2**–**7**.

After complete utilization of PhSeH and formation of product **1a** (40 min), benzenethiol PhSH was selected next

dx.doi.org/10.1021/ja210596w | J. Am. Chem. Soc. 2012, 134, 6637−6649

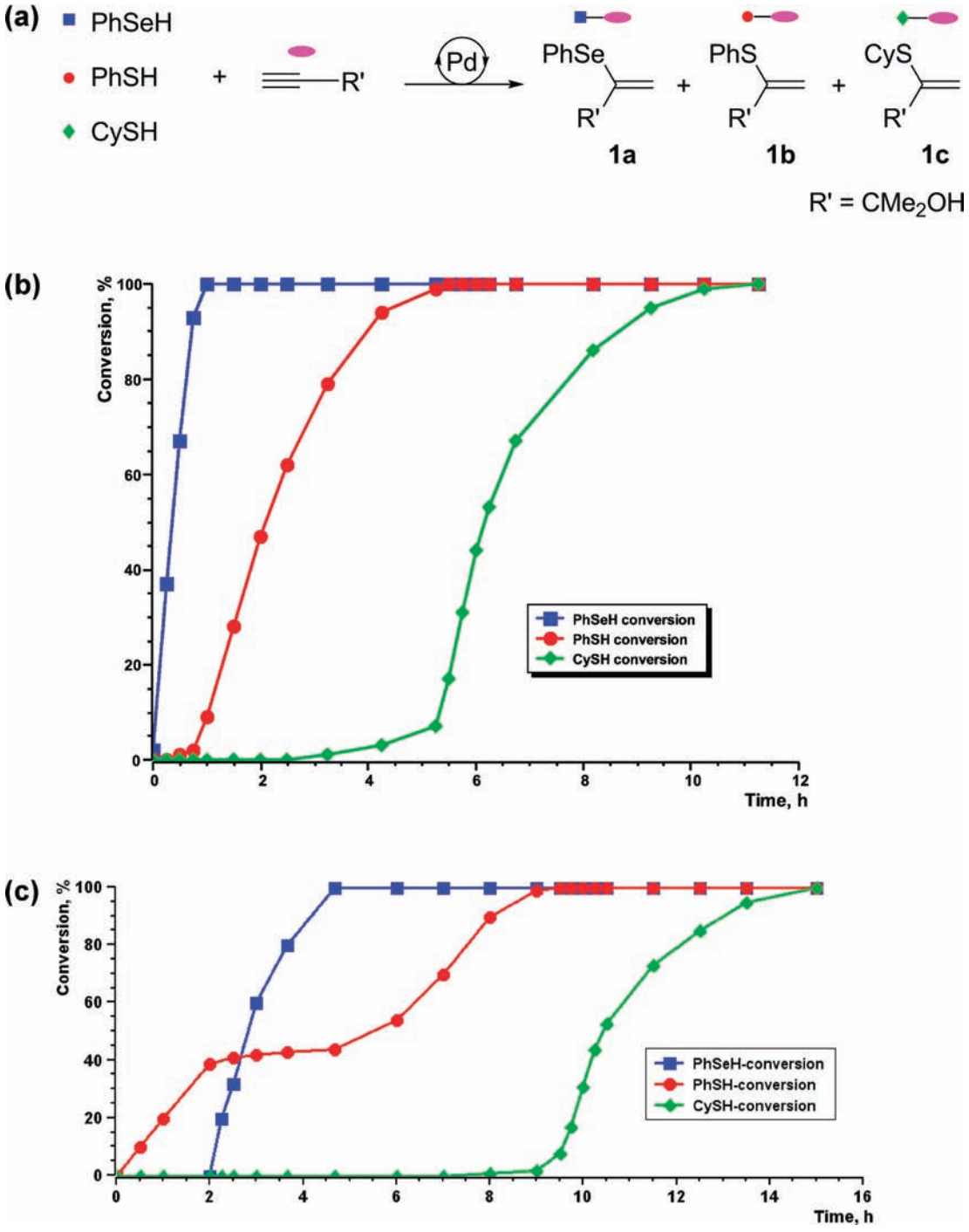

Figure 1. (a) Reaction of PhSeH, PhSH, and CySH with 2-methyl-3-butyn-2-ol, (b) NMR monitoring of the reaction starting with three-component PhSeH/PhSH/CySH mixture, (c) NMR monitoring of the reaction starting with binary PhSH/CySH mixture and with PhSeH added after 2 h of the reaction.

by the catalyst for addition to the alkyne that led to synthesis of product **1b** (Figure 1b). The latter reaction was completed in 4 h. At the third stage, which started after complete usage of PhSH, the CySH was picked-up for reaction with the alkyne that led to formation of product **1c** (Figure 1b). At the second and third stages of the transformation, again, compounds **1b** and **1c** were the only products; no other byproduct, such as **2**–**7**, were obtained. Thus, the developed heterogeneous catalyst exhibits exceptional selectivity to the three-component mixture of PhSeH/PhSH/CySH = 1:1:1, and exclusively promotes the formation of Markovnikov-type products **1a, 1b** and **1c**, respectively. No other byproduct, including mixture of anti-Markovnikov products, were obtained.

Under the same conditions the catalytic addition reaction was also carried out for the binary mixtures PhSeH/PhSH, PhSeH/CySH, and PhSH/CySH. In all three cases the same order in the reactivity (and capture) was observed: PhSeH > PhSH > CySH. It is essential to note that the order of chalcogen species removal from the mixture matches their

dx.doi.org/10.1021/ja210596w | J. Am. Chem. Soc. 2012, 134, 6637–6649

Table 1. Temperature and Yields for Reaction of Different Alkynes with PhSeH/PhSH/CySH Mixture[a]

Entry	Alkyne	1a		1b		1c	
		T, °C	Yield, %	T, °C	Yield, %	T, °C	Yield, %
1	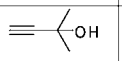	80	99	100	99	120	98
2	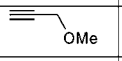	80	99	100	98	120	96
3	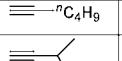	80	99	100	97	120	97
4	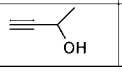	80	99	100	98	120	96

[a]R′ = $C(Me)_2OH$, CH_2OMe, $^nC_4H_9$, $CH(OH)CH_3$ for entries 1−4, respectively (Figure 1a).

toxicity; the more toxic is the component, the earlier the removal from the mixture takes place.

The above presented results clearly demonstrate that, although the reagents PhSeH, PhSH, and CySH were presented as a mixture, the products **1a**, **1b**, and **1c**, respectively, can be obtained in a pure form. Comparison of experimental conditions needed for full conversion, 40 min at 80 °C for PhSeH, 4 h at 100 °C for PhSH, and 8 h at 120 °C for CySH, clearly emphasizes high potential of the used Pd-based catalyst to distinguish the reagents of similar nature.

The scope of the reaction was verified with different alkynes and in all studied cases the stepwise reaction with excellent selectivity was observed (Table 1). Only one of the components of PhSeH/PhSH/CySH mixture was reacted at a time with alkyne. Similar kinetic curves were observed for all studied alkynes independent of substituent (R′) induced differences in reactivity. The final yields of products **1a**−**1c** were in the range of 96−99% (Table 1).

In summary, the developed catalytic system has shown (i) exceptional reagent-specific selectivity toward chalcogen species; (ii) excellent selectivity and high product yield in the addition reaction, without formation of any byproduct; and (iii) easy availability of catalyst precursor with smart recovery after the reaction (heterogeneous catalysis).

2.2. Dynamically Changed Mixture of Reagents and Dynamic Range Test. As a crucial test of the designed catalytic system, a dynamically changed mixture of reagents was investigated (Figure 1c). The reaction was initiated with the PhSH/CySH (1:1) two-component mixture. As it was expected, at first, the selective capture of PhSH by the catalyst gave product **1b** upon reaction with the alkyne. During this process (after 2 h) the PhSeH was added to the reaction mixture. As a result, immediately after the PhSeH addition, the formation of product **1b** was stopped and the formation of the product **1a** was started without any visible induction period. After complete utilization of PhSeH (~3 h) the use of PhSH by the catalytic system has resumed and led to production of **1b**. Finally, after complete usage of PhSH (totally ~9 h), the remaining component of the mixture, CySH, was consumed to produce **1c**. As already noted, no other byproducts were detected in the course of the reaction. The dynamic nature of the catalytic system implies possible application in flow conditions, where a varying content of the mixture may be expected. No additional manipulations with the catalytic system were needed; the catalyst was adaptively tuned upon interaction with reaction media and showed a rapid response reflecting the content of the mixture. Remarkably, the order in the reactivity and chalcogen species removal from the mixture, i.e. PhSeH > PhSH > CySH, was preserved.

In the above-presented experiments we used the equimolar mixtures of chalcogen derivatives. In order to determine the minimal amount of a mixture component that can be selectively captured on a large background concentration of another reactive species, we performed dynamic range tests. These tests have shown that phenylselenol was completely extracted from the PhSeH:PhSH binary mixture that led to the quantitative yield of **1a** in 2.0−2.0 × 10^{-3} M concentration range of PhSeH and under constant background concentration of PhSH = 2.0 M. Even at 4 orders of magnitude difference in the concentrations, C_{PhSeH} = 2.0 × 10^{-4} M and C_{PhSH} = 2.0 M, the minor component of PhSeH addition was fully detected by NMR after the reaction. This gives an excellent dynamic range of at least 1:10000 for the developed catalytic system. The studies with further decrease in the concentration of PhSeH were not feasible because the sensitivity limit of the used analytic method was already reached.

2.3. The Nature of the Catalytic Species. Our extensive analysis of the nature of active catalyst generated after addition of $Pd(OAc)_2$ as a catalyst precursor to a mixture of chalcogen reagents RZH (Z = S and Se) and acetylenic hydrocarbons revealed heterogeneous nature of the studied system. Insoluble metal-containing particles have been formed shortly after reacting of $Pd(OAc)_2$ with thiols or selenol. Filtering out the metal-containing solids resulted in complete loss of the catalytic activity, indicating a very minor (if any) metal-containing species in solution.

The isolated catalyst was characterized using field-emission scanning electron microscopy technique (FE-SEM). Approximately round-shaped particles with sizes in the range of 30−60 nm were observed (Figure 2). The particles did not agglomerate into the range of microscale sizes, and the edges between the individual nanoparticles were clearly resolved (Figure 2). The nanoparticles were self-assembled under simple conditions in solution upon contact of $Pd(OAc)_2$ with the reagents: alkyne and RZH. Neither stabilizers/surfactants nor any dedicated support were required to keep the nanosized structural organization of the catalyst. Thus, the system demonstrated outstanding practical advantages for easy and convenient in situ catalyst formation without the need of complicated and expensive catalyst preparation procedures utilized for making supported heterogeneous catalysts.

Microanalysis of the precipitate formed at the first stage of reaction in the three-component system PhSeH/PhSH/CySH (Figure 1b) showed the initial catalyst composition to be $[Pd(SePh)_2]_n$ (entry 1, Table 2): no sulfur in the active catalyst composition was detected. It should be pointed out that the microanalysis gave overall information about bulk catalyst (both core and surface). Therefore, we performed a separate analysis

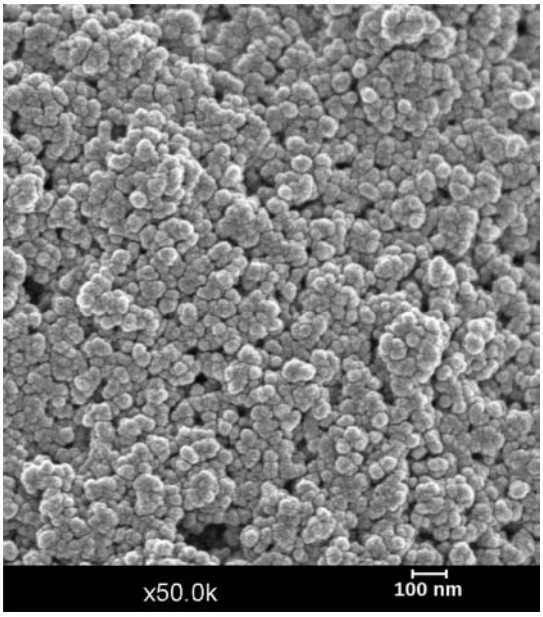

Figure 2. FE-SEM of the $[Pd(ZR)_2]_n$ catalyst particles isolated from the reaction mixture (50000× magnification; 100-nm scale bar is shown).

of the catalyst surface by utilizing EDS-SEM technique and confirmed the presence of the SePh groups on the surface (entry 1, Table 2). Uniform distribution of Se on the surface was detected by recording X-ray maps in the EDS-SEM study.

In contrast, the active catalyst isolated after 3 h of reaction, i.e. after the consumption of all selenols in the PhSeH/PhSH/CySH mixture [this stage of the reaction corresponds to the PhSH capture and addition (Figure 1b)], contained 3−6% of sulfur, and the amount of selenium decreased. These findings indicate that some part of the SePh groups in the original $[Pd(SePh)_2]_n$ catalyst has been replaced by SPh groups. The corresponding EDS-SEM study confirmed the presence of the SPh groups on the surface (entry 2, Table 2). Thus, these experiments suggest an exchange of SePh groups located at the surface of the original $[Pd(SePh)_2]_n$ catalyst with SPh groups.

At the third stage of the reaction that corresponds to the selective CySH capture from the mixture and **1c** formation, further modification of the surface was observed, and attachment of the SCy groups took place (entry 3, Table 2, and Figure 1, b and c).

On the basis of the presented data one can conclude that, at the first stage of the reaction in the three-component system PhSeH/PhSH/CySH (Figure 1b), the $[Pd(SePh)_2]_n$ (entry 1, Table 2) is the active catalyst. At the second and third stages of this reaction corresponding to the selective PhSH and CySH capture from the mixture, respectively, the exchange of SePh groups (located at the surface of the catalyst) with SPh and SCy groups occurs. Intriguingly, these overall experiments indicate the SPh coordination to the catalyst surface to be more preferable than the SCy groups coordination.

2.4. Comparison with Noncatalytic Conditions and with the Homogeneous Catalytic System. In order to demonstrate superior properties of the newly developed catalytic system we have compared its performance in the capture and addition of chalcogen species to alkyne with those reactions performed under *no metal catalyst* and *homogeneous metal catalyst* conditions. Our experiments under *no metal catalyst* conditions did not lead to the formation of desired (industrially) product **1**; instead, the formation of a mixture of compounds **2** and **3** was observed. These results well agree with those reported for addition of thiols and selenols to alkynes under radical and nucleophilic conditions.[18,19]

Experiments under the *homogeneous metal catalyst* conditions were performed by using an excess of phosphine ligand (below called as a Pd/PPh_3 catalyst), which prevented precipitation of metal particles and kept the metal species in the solution. ^{31}P and ^{1}H NMR study of the nature of the active catalyst under the *homogeneous metal catalyst* conditions identified the formation of $[Pd(ZR)_2(PPh_3)_2]$ complexes (Z = S, Se) in agreement with previous studies.[20] The reaction of PhSeH (or PhSH) as an individual reagent with the alkyne, performed under the Pd/PPh_3 catalyst conditions, resulted in a mixture of vinylic products containing one and two ZPh groups (**1**−**4**; Z = S and Se). The results are even worse for the two-component PhSeH/PhSH (1:1) mixture that reacted with the alkyne under the same Pd/PPh_3 catalyst. For this reaction, we have found a multicomponent mixture of products containing vinylic compounds with one and two chalcogen groups (**1**−**4**), as well as the alkene **5**. Furthermore, the formation of compound **4**, containing both SePh and SPh groups, was also observed. In other words, addition of thiols and selenols (and related systems) to alkyne under the *homogeneous metal catalyst* conditions led to the formation of a mixture of various products without desired selectivity.

Thus, homogeneous and heterogeneous catalytic systems reported in this article contain the same structural unit—$Pd(ZR)_2$; however, the heterogeneous Pd catalyst shows superiority in reactivity and selectivity compared to the homogeneous catalyst.

Having the above presented results in our hands, we elucidate below the mechanism and the key factors controlling selective capture and addition of chalcogen species to alkyne exclusively via the formation of Markovnikov-type products. As a first step, we have studied the structure and stability of the catalyst $[Pd(ZR)_2]_n$ for Z = S and Se, R = Me, and n = 1−9 by utilizing computational tools.

2.5. Computed Structure and Stability of the $[Pd(ZR)_2]_n$ Clusters, for Z = S and Se, R = Me, and n = 1−9. Reaction of two RZH molecules with the precursor of the

Table 2. Microanalysis and EDS-SEM Study of the Catalytic Particles at Various Stages[a]

			microanalysis,[c] %			EDS-SEM,[c] %		
entry	step[b]	catalyst	Pd	Se	S	Pd	Se	S
1	**A**	$[Pd(SePh)_2]_n$	25.1	37.3	0.0	25.0	38.2	0.0
2	**B**	$[Pd_n(SePh)_{2n-x}(SPh)_x]$	26.2	30.1	3.5	26.1	28.3	5.9
3	**C**	$[Pd_n(SePh)_{2n-x}(SR)_x]$	26.3	29.8	3.9	26.0	27.7	6.5

[a]Calculated values (%) $[Pd(SePh)_2]_n$: Pd 25.4; Se 37.7; C 34.5; H 2.4; $[Pd(SPh)_2]_n$: Pd 32.8; S 19.7; C 44.4; H 3.10; $[Pd(SCy)_2]_n$: Pd 31.6; S 19.0; C 42.8; H 6.6. [b]**A** - reaction with PhSeH, **B** - reaction with PhSH, **C** - reaction with CySH (see Figure 1b). [c]Estimated error = ±0.5%.

dx.doi.org/10.1021/ja210596w | *J. Am. Chem. Soc.* 2012, 134, 6637−6649

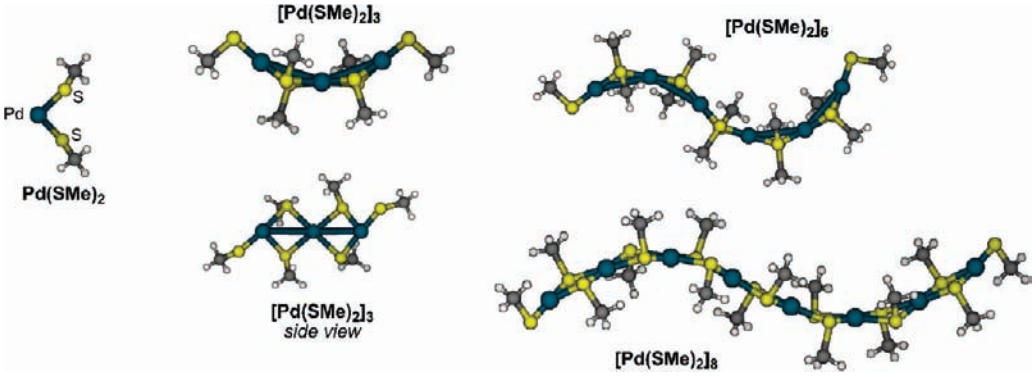

Figure 3. Optimized structures of $[Pd(SR)_2]_n$ chains at B3LYP level for n = 1, 3, 6, and 8 (atom colors are shown for the mononuclear derivative).[22].

Scheme 3. Formation of Polynuclear Metal Species from Pd(II) Salt

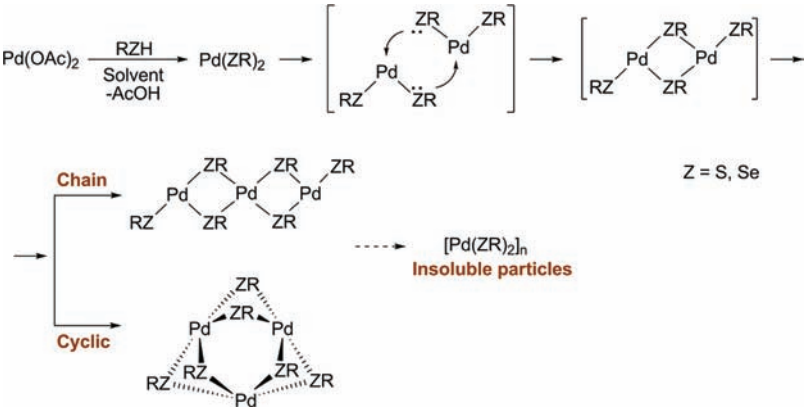

catalyst, $Pd(OAc)_2$, leads to formation of $Pd(ZR)_2$ complex with a bent structure (see Figure 3; optimized geometries of all reported structures in this paper are presented in the Supporting Information). The overall reaction $Pd(OAc)_2$ + 2HZR → $Pd(ZR)_2$ + AcOH is calculated to be exothermic by −50.0 (−63.3) kcal/mol (throughout this paper, the energy values given without parentheses are for Z = S, while the values given in parentheses are for Z = Se) on free energy surface and expected to proceed with a small energy barrier. Under experimental conditions this step of the reaction, i.e. the substitution of the OAc ligand by RZH and release of free AcOH, was confirmed by ^{1}H and ^{13}C NMR measurements.

If the $Pd(ZR)_2$ complex is formed in the absence of phosphine or other strong ligands,[21] then a lone-pair of the coordinated chalcogen atom reacts with the second Pd center to form a dimeric species (see Scheme 3). For the $[Pd(ZR)_2]_2$ dimer, the rhombic structure with two bridging (μ_2, we also call them "core" ligands) and two terminal (μ_1, we also call them "surface" ligands) ZR ligands is found to be energetically the most stable. The calculated free energy of dimerization is −28.5 (−31.8) kcal/mol. The averaged Pd−Z bond energy ($\Delta G/m$) [as an oligomerization energy divided by number of Pd−Z bonds, m, which is equal to $4n$ for cyclic and $4n - 2$ for linear complexes] is found to be 6.9 (7.4) kcal/mol in $[Pd(ZR)_2]_2$ dimer (see Table 3). Subsequent addition of the $Pd(ZR)_2$ units is expected to lead to the formation of the $[Pd(ZR)_2]_n$ species, which at a certain point (i.e., at certain n) would become insoluble and precipitate. Indeed, our experimental studies of the reaction of $Pd(OAc)_2$ with a mixture of chalcogen derivatives confirmed that this process does take place under the studied reaction conditions, and the resultant metal particles of general formula $[Pd(ZR)_2]_n$ (see Table 2) are insoluble. Our computational studies show that the clusters with more than two $Pd(ZR)_2$ units may have at least two stable structures—chain and cyclic (see Scheme 3 for reactions; and Figures 3, 4 for optimized structures).

Table 3. Calculated Pd−Z Bond Energy for Chain and Cyclic $[Pd(ZR)_2]_n$ Palladium Complexes (in kcal/mol)[a,b]

	chain complexes		cyclic complexes	
n	$\Delta H/m$	$\Delta G/m$	$\Delta H/m$	$\Delta G/m$
2	−6.9 (−7.4)	−4.8 (−5.3)	–	–
3	−9.1 (−9.5)	−6.4 (−6.9)	−7.9 (−8.7)	−5.1 (−6.0)
4	−9.9 (−10.3)	−7.0 (−7.6)	−11.0 (−11.5)	−7.9 (−8.4)
5	−10.5 (−10.8)	−7.4 (−7.8)	−11.7 (−12.1)	−8.4 (−8.9)
6	−10.7 (−11.1)	−7.6 (−8.1)	−12.1 (−12.5)	−8.8 (−9.3)
7	−11.0 (−11.3)	−7.7 (−8.1)	−12.1 (−12.4)	−8.7 (−9.2)
8	−11.1 (−11.5)	−7.9 (−8.3)	−12.2 (−12.5)	−8.9 (−9.4)
9	−11.2 (−11.6)	−7.9 (−8.4)	−12.1 (−12.5)	−8.8 (−9.2)

[a]The values without parentheses correspond to Z = S, the values in parentheses correspond to Z = Se. [b]Averaged $\Delta H/m$ and $\Delta G/m$ values are given, where ΔH and ΔG were calculated for the n $Pd(ZMe)_2$ → $[Pd(ZMe)_2]_n$ reaction and m is the number of Pd−Z bonds ($m = 4n$ for cyclic and $m = 4n - 2$ for linear complexes, respectively).

As seen in Table 3, the chain structure is more stable than the cyclic one, only for n = 3, where the calculated averaged Pd−Z bond free energies ($\Delta G/m$) are 6.4 (6.9) and 5.1 (6.0) kcal/mol, respectively. However, for $n \geq 4$, the calculated $\Delta G/m$ value become larger for the cyclic structure than for the chain one, indicating the cyclic structures to be energetically more

dx.doi.org/10.1021/ja210596w | J. Am. Chem. Soc. 2012, 134, 6637−6649

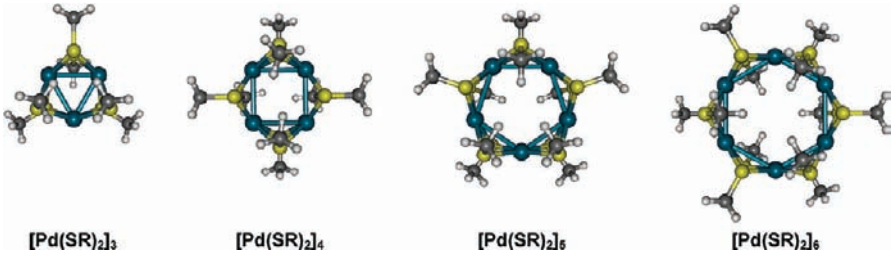

Figure 4. Optimized structures of cyclic $[Pd(SR)_2]_n$ complexes at B3LYP level with n = 3−6.[22].

Scheme 4. Schematic Presentation of the Alkyne Insertion into Terminal Pd−(μ_1-ZR) and Bridging Pd−(μ_2-Z′R) Bonds (Z, Z′ = S and Se) in Binuclear Complexes

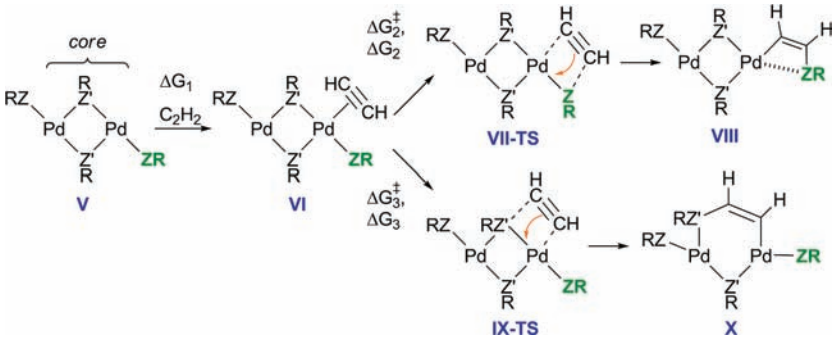

favorable than chain structures. Importantly, the Pd−Z bond energies show different trends for the chain and cyclic complexes. In the cyclic complexes the Pd−Z energy has converged at n = 6 to a value of 8.8 (9.3) kcal/mol and did not change noticeably afterward (Table 3), whereas in the chain complexes it monotonously increases and may finally reach a value similar (or larger) to that for cyclic structures at large n's. The calculated $\Delta G/m$ value of Pd−Z bond is 7.9 (8.4) kcal/mol at n = 9.

It is important to state that the $\Delta G/m$ values are found to be 0.3−0.5 kcal/mol larger for the Pd−Se bonds than the Pd−S bonds (see Table 3). This indicates that in the three-component mixture of PhSeH/PhSH/CySH = 1:1:1, selenol will react first with Pd-centers before sulfur-containing species. This finding is in a good agreement with our experimental data.

On the basis of these findings we conclude that at lower numbers of n (but higher than n = 3) the most stable structure of the $[Pd(ZR)_2]_n$ cluster is its cyclic conformer, while at larger numbers of n the chain structure may become energetically as stable as or even more stable than the cyclic structure. It should be emphasized that in cyclic structures all Pd centers are equivalent and contain only μ_2-ZR ligands. Alternatively, in chain structures two different types of metal centers exist: two unsaturated Pd-centers at the ends of the chain each with one μ_1-ZR ligand and one coordination vacancy, and n − 2 saturated Pd-centers with four μ_2-ZR ligands each. Smaller averaged bond energy (Table 3) in the case of chain structures may be explained by the presence of such unsaturated centers.

Armed with the above presented knowledge on the structure of $[Pd(ZR)_2]_n$ compounds, below we intend to elucidate the reaction mechanism and the factors controlling chalcogen addition to alkyne. At first, we elaborate the reactivity of the chain structure of $[Pd(ZR)_2]_n$ compound because it has two different chalcogen groups, terminal μ_1-ZR and bridging μ_2-ZR, while the cyclic structure has only the bridging μ_2-ZR ligands. Consequently, the structural motif of chain structure provides better opportunity to elucidate reactions of both μ_1-ZR and μ_2-ZR ligands with alkyne. We believe that the obtained knowledge on reactivity of μ_2-ZR ligands in the chain structure will be transferable to the cyclic $[Pd(ZR)_2]_n$ compounds.

2.6. Difference in Reactivity of the μ_1-(Terminal) and μ_2-(Bridging) ZR Groups. Calculations revealed critical difference in reactivity of μ_1-(terminal) and μ_2-(bridging) ZR (R = Me) groups of binuclear complex **V** (Scheme 4), a model of active catalyst, with alkyne (i.e., C_2H_2).[23] The first step of the reaction is the alkyne coordination to one of the coordinatively unsaturated Pd-centers to form a weakly bound π-complex **VI**.[24] In complex **VI** the coordinated alkyne ligand can react either with μ_1-ZR (via the **VI→VII-TS→VIII** pathway) or with μ_2-ZR ligand (via the **VI→IX-TS→X** pathway). At first, we rationalize the difference in reactivity of the μ_1- and μ_2-coordinated chalcogen groups ZR toward alkynes (i.e., either surface or core ZR ligands, respectively; where Z = S and Se). As seen in Table 4, the alkyne coordination to one of the coordinatively unsaturated Pd-centers of **V** to form weakly bound π-complex **VI** is calculated to be 1.4 (1.8) kcal/mol exothermic (based on the free energies).[24] For Z = S, the alkyne insertion into the terminal (i.e., surface) Pd−(μ_1-SR) bond, occurring via the **VI→VII-TS→VIII** pathway, requires $\Delta G_2^{\ddagger}$ = 5.9 kcal/mol activation barrier at the transition state

Table 4. Free Energy Parameters (ΔG, in kcal/mol) for the Model Alkyne Insertion Reaction V + C_2H_2 (see Scheme 4), Calculated at the B3LYP Level of Theory

	sulfur core (Z′ = S)		selenium core (Z′ = Se)	
point	Z = S	Z = Se	Z = S	Z = Se
ΔG_1 **V→VI**	−1.4	−3.2	−1.8	−1.8
$\Delta G^{\ddagger}_2$ **VI→VII-TS**	5.9	6.8	7.8	7.3
ΔG_2 **VI→VIII**	−19.7	−15.1	−17.6	−14.3
$\Delta G^{\ddagger}_3$ **VI→ IX-TS**	20.5	22.6	21.8	21.7
ΔG_3 **VI →X**	5.5	6.5	10.0	10.0

dx.doi.org/10.1021/ja210596w | J. Am. Chem. Soc. 2012, 134, 6637−6649

VII-TS and is exothermic by $\Delta G_2 = -19.7$ kcal/mol. Whereas the alkyne insertion into the bridging (i.e., core) Pd−(μ_2-SR) bond, occurring via the **VI→IX-TS→X** pathway, requires a much larger, $\Delta G_3^{\ddagger} = 20.5$ kcal/mol, energy barrier at the transition state **IX-TS**, and is $\Delta G_3 = 5.5$ kcal/mol endothermic. Similarly, for Z = Se, the alkyne insertion into the terminal Pd−(μ_1-SeR) bond occurring via the **VI→VII-TS→VIII** pathway requires $\Delta G_2^{\ddagger} = 7.3$ kcal/mol activation barrier at **VII-TS**, and is exothermic by $\Delta G_2 = -14.3$ kcal/mol. However, the alkyne insertion into the bridging Pd−(μ_2-SeR) bond occurring via the **VI→IX-TS→X** pathway requires a much larger, $\Delta G_3^{\ddagger} = 21.7$ kcal/mol, energy barrier at **IX-TS**, and is endothermic with $\Delta G_3 = 10.0$ kcal/mol. Comparison of these energetics between Z = S and Z = Se shows that for selenium compounds, the calculated barriers are slightly larger and overall reactions are less exothermic (or more endothermic) than those for sulfur compounds. This trend is consistent with the difference in the bonding energies of Pd−Se and Pd−S bonds: Pd−Se is slightly stronger than Pd−S.

Thus, the insertion of alkyne into the Pd−(μ_1-ZR) and Pd−(μ_2-ZR) bonds of $[Pd(ZR)_2]_2$ is dramatically different and preferably proceeds via the insertion into Pd−(μ_1-ZR) bond. As seen in Scheme 4, in binuclear complex $[Pd(ZR)_2]_2$ (as well as possibly in all other chain $[Pd(ZR)_2]_n$ compounds) only one ZR group in each Pd-center located at the ends of the chain is reactive toward alkyne. With such a difference in reactivity of the coordinated ZR groups in $[Pd(ZR)_2]_n$ (chain compounds) we should expect the formation of only vinylic product **1**: the formation of product **4** with two ZR groups is not feasible.[25]

On the basis of the above-presented analyses for the $[Pd(ZR)_2]_2$ systems with the same ZR (either SR or SeR) groups on the both core (μ_2-) and surface (μ_1-) positions, we conclude that the weaker Pd−Z bond the smaller energy barrier, and the more exothermic is alkyne insertion into Pd−Z bond. Now, we wish to elucidate the effect of the nature of core μ_2-ZR groups to the reactivity of the surface μ_1-ZR groups. As seen in Table 4, replacement of all μ_2-SR core ligands in $[Pd(SR)_2]_2$ by μ_2-SeR (i.e., S-to-Se replacement) has slightly *increased* the calculated energy barriers and *reduced* exothermicity of alkyne insertion into the Pd−(μ_1-SR) bond. On the contrary, replacement of all core μ_2-SeR ligands in $[Pd(SeR)_2]_2$ by μ_2-SR (i.e., Se-to-S replacement) has slightly *reduced* the energy barrier and *increased* the exothermicity of the reaction of alkyne insertion into the Pd−(μ_1-SeR) bond. The obtained effect of the nature of the core (μ_2-ZR group) on the reactivity of the surface Pd−(μ_1-ZR) bond could be, again, explained in terms of the Pd−Z bonding energy. Indeed, as we have discussed above (see Table 3), the $\Delta G/m$ values for the Pd−Se bond (averaged, 0.3−0.5 kcal/mol) are slightly stronger than those for the Pd−S bond, which allows us to conclude that the weaker bonding is observed in the core, and the easier alkyne insertion involves the terminal Pd−(μ_1-ZR) bond.

Furthermore, as seen in Table 4, if the terminal Pd−(μ_1-ZR) bond is not stronger than the core Pd−(μ_2-ZR) bond, then it has no effect on the reactivity of the alkyne insertion into the core Pd−(μ_2-ZR) (Z = S and Se) bonds. On the contrary, replacement of stronger terminal Pd−(μ_1-SeR) bonds by the weaker Pd−(μ_1-SR) bonds reduces both the barrier and the endothermicity of the alkyne insertion into the core Pd−(μ_2-SR) bond.

Thus, from extensive computational studies, we have shown that: (a) the energetically most favorable structure of the $[Pd(ZR)_2]_n$ compound *for smaller n's* is a cyclic structure. *For larger n's,* the chain structure of $[Pd(ZR)_2]_n$ becomes energetically closer to the cyclic structure and is accessible for alkyne addition reaction; (b) reactivity of the μ_1-(terminal) and μ_2-(bridging) ZR groups (Z = S and Se, R = Me) are very different: the terminal (or surface) μ_1-ZR groups are significantly more reactive than the bridging (or core) μ_2-ZR groups, and (c) the unique feature of the cyclic complexes is the absence of the η^1-SR groups. If our results on relative reactivity of the μ_1-SR and μ_2-SR groups discussed above are correct, then the cyclic complexes should be totally unreactive toward alkynes and can be prepared and isolated, at least for smaller *n*'s.

On the basis of these computational findings, we propose the following plausible mechanism of the selective capture and addition of various chalcogen groups to alkyne (Scheme 5).

Scheme 5. Proposed reaction mechanism of catalyst formation and the plausible catalytic cycle

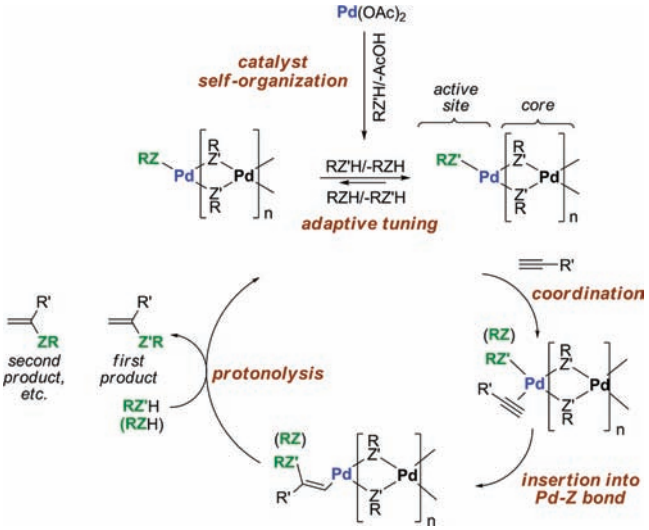

The catalytic cycle starts with the formation of active catalyst $[Pd(ZR)_2]_n$ from the $Pd(OAc)_2$ precursor and chalcogen derivatives. Formation of the metal organochalcogen particles was confirmed by EDS-SEM and microanalysis (Table 2). For smaller *n*'s, the metal organochalcogen particles contain only inactive core (μ_2-SR) ligands and, therefore, are inert and can be isolated (see below). However, for larger *n*'s, the chain structure of the $[Pd(ZR)_2]_n$ compounds containing both inactive μ_2-ZR and reactive μ_1-ZR groups becomes energetically accessible. Within such an arrangement of the active catalyst $[Pd(ZR)_2]_n$ the further transformations leading to product **1** are alkyne coordination, alkyne insertion into the terminal Pd−(μ_1-ZR) bond, and protonolysis. Since the averaged Pd−SeR bond energy is calculated to be slightly larger than the averaged value for the Pd−SR bond, the catalytic system is first expected to utilize the selenols before thiols, which is in a good agreement with the above-presented experiments.

Further proof for this mechanism proposed on the basis of the computational studies can be experimental evidence such as preparation and investigation of reactivity of the cyclic $[Pd(ZR)_2]_n$ compounds.

2.7. Proof of Concept: Unreactive μ_2-SR Groups. Gratifyingly, unambiguous confirmation of the above proposed mechanism was obtained by successful preparation of the cyclic complex $[Pd(S^nHex)_2]_6$ (**8**), the structure of which was

dx.doi.org/10.1021/ja210596w | J. Am. Chem. Soc. 2012, 134, 6637−6649

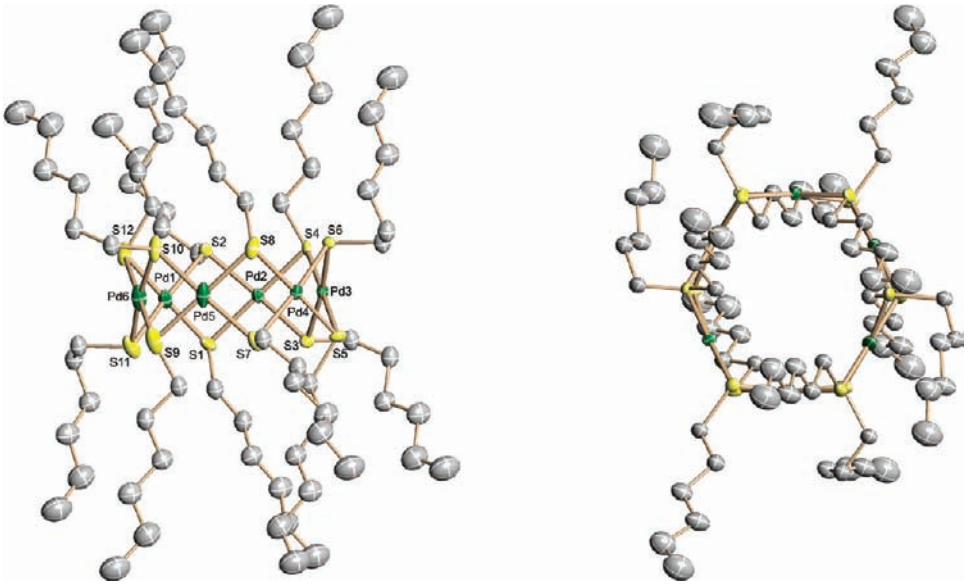

Figure 5. Molecular structure of cyclic $[Pd(S^nHex)_2]_6$ complex (**8**) determined by X-ray analysis (50% ellipsoids; side view and top view). One of the two crystallographically independent molecules is presented (hydrogen atoms are omitted for clarity).

Scheme 6. Surface Groups Exchange and Alkyne Insertions in Multicomponent Mixtureddd

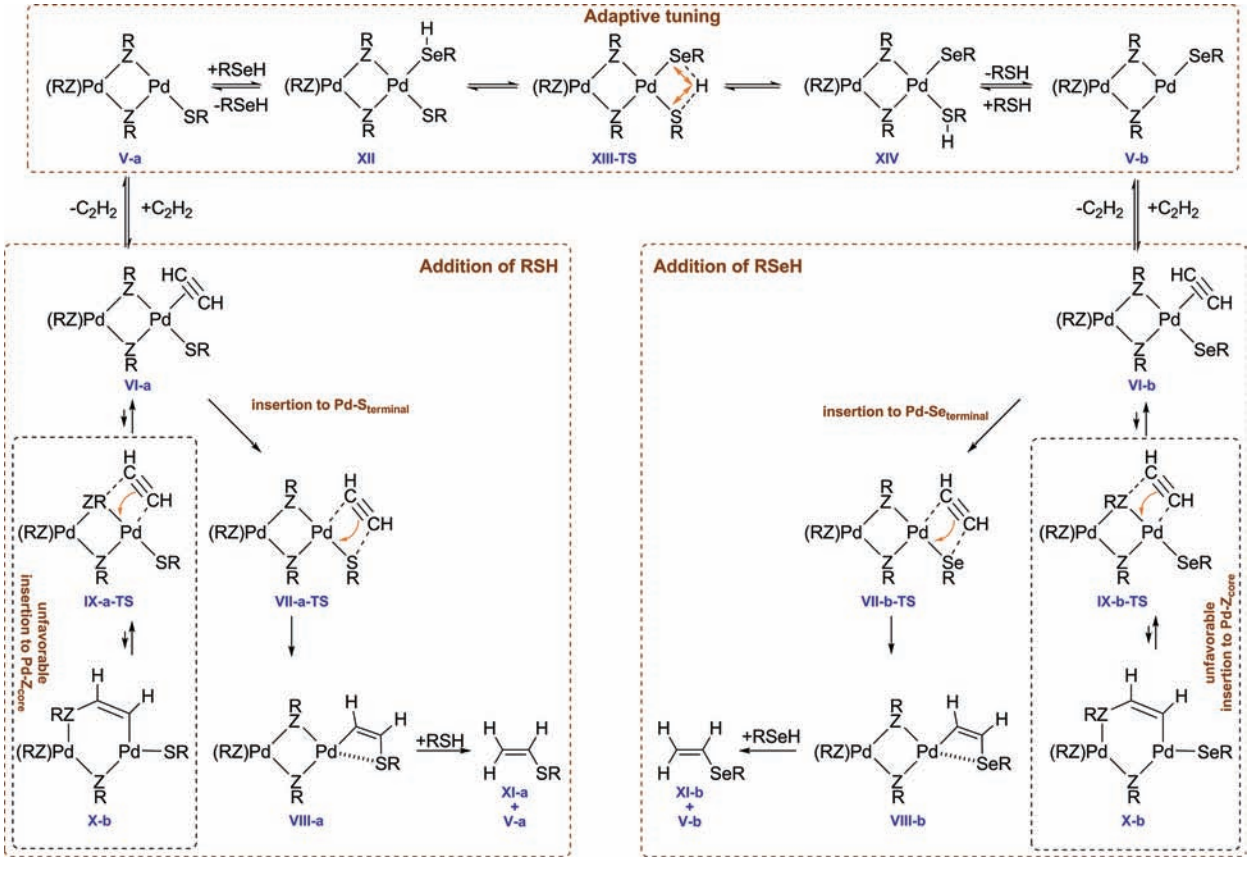

established by a single crystal X-ray diffraction analysis (Figure 5) in the solid state. Solution structure of the complex was confirmed by ^1H, ^{13}C NMR and complete line assignment was carried out using 1D selective TOCSY and 2D HSQC NMR (see Supporting Information for details). Hexanuclear nature of complex **8** in solution was confirmed by ESI-MS measurements.

The crystal of **8** contained two crystallographically independent molecules with similar geometries (see Supporting Information for details). As seen in Figure 5, the Pd(II) thiolate complex **8** has a tiara-like structure. In each cluster, the six palladium atoms form a nearly planar hexagonal ring with the average Pd···Pd distances of 3.112(2) and 3.115(2) Å, for the two crystallographically independent molecules. Each palladium atom is coordinated to four sulfur atoms with an approximately

dx.doi.org/10.1021/ja210596w | J. Am. Chem. Soc. 2012, 134, 6637–6649

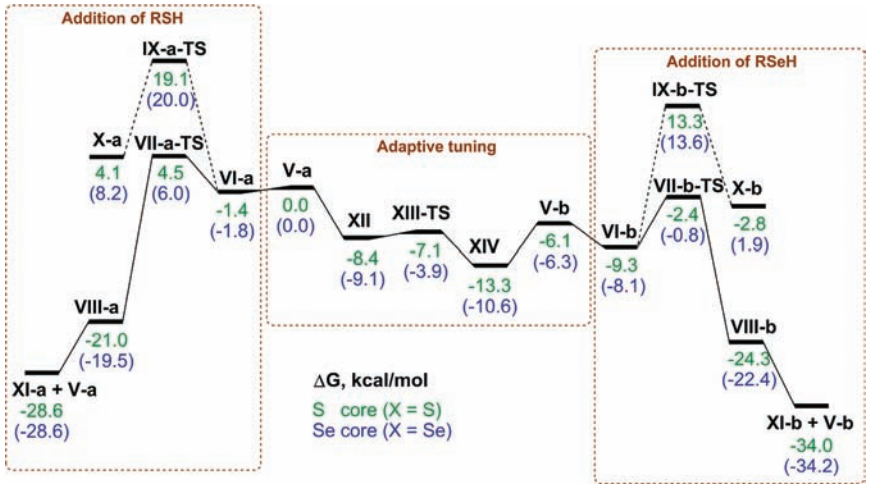

Figure 6. Calculated ΔG energy surface of the reaction in multicomponent mixture; for the sulfur core the numbers are in green, for the selenium core the numbers are in blue (see Scheme 6 for structures).

square-planar configuration (the S−Pd−S bond angles vary within 81.0(1)−98.9(1) and 81.4(1)−98.6(1)°, for the two crystallographically independent molecules), and the average Pd−S bond lengths are 2.313(4) and 2.320(4) Å, for the two crystallographically independent molecules. The 12 sulfur atoms form two S_6 hexagons parallel to the central Pd_6 ring from both sides. The dihedral angles between the PdS_4 coordination planes range within 115.19(6)−126.39(6) and 115.77(7)−126.53(7)°, for the two crystallographically independent molecules. The average S···S distances in S_6 rings are 3.489(6), 3.498(6) and 3.503(6), 3.493(6) Å, for the two crystallographically independent molecules, indicating no S−S bond. Such a triple-layered tiara-like structure is about 3.06 and 3.05 Å in height for the two crystallographically independent molecules, with a symmetry close to D_{6h} (see Supporting Information for detailed structure data). The S−C bonds are alternately directed either parallel or perpendicular to the S_6 rings (Figure 5, right). Such an arrangement is attributed to the steric repulsion and has been found in other analogous $[Pd(SR)_2]_6$ (R = CH_3,[26a] CH_2CH_3,[26b] $(CH_2)_{11}CH_3$,[26c] CH_2COOCH_3[26d]) complexes. However, regardless of the S−C bonds, the long terminal carbon chains are disposed roughly parallel to each other (Figure 5). This disposition is apparently explained by the crystal packing of molecules, which is stacked along the *b*-axis.

The symmetrical cyclic structure of **8** in solution was confirmed by ^1H and ^{13}C NMR (see Supporting Information). Importantly, it was found that complex **8** is totally inactive toward alkynes. Addition of alkyne to **8** produces neither **1** nor **4**, even after continuous heating at 100 °C. Thus, the synthesis of the complex **8** and its inactivity with alkyne clearly confirms our theoretical predictions on the stability of cyclic derivatives for smaller *n*'s and unreactive nature of the μ_2-SR groups.

2.8. Adaptive Tuning of the Catalyst. An important issue, which we address in this paper, is the nature of adaptive tuning of the catalyst (Scheme 6). Obviously, the relative reactivity of terminal Pd−(μ_1-ZR) bonds and the effect of the core μ_2-ZR ligands on their reactivity are not responsible for the observed adaptive tuning of the catalyst. To obtain insight into the nature of adaptive tuning we have constructed the potential energy profile of the reaction (Figure 6). The studied system mimics the experimental conditions when the mixture of RSeH/RSH was used as the initial reagent in the reaction with alkyne. The calculations with selenium and sulfur cores were carried out to model the experimental reaction showed in Figure 1 b and c, respectively.

A seen in Scheme 6, the reaction leading to the formation of sulfur product **XI-a** (left-hand-side of the Scheme 6 and Figure 6) starts from the complex **V-a** and proceeds via alkyne insertion transition state **VII-a-TS**. In a similar pathway, the reaction leading to the formation of selenium product **XI-b** (right-hand-side of the Scheme 6 and Figure 6) starts from the complex **V-b** and proceeds via alkyne insertion transition state **VII-b-TS**.

Surprisingly, we have found that μ_1-coordinated chalcogen groups can exchange very easily at the catalyst active site (the middle part of Figure 6 and the top part of Scheme 6). Coordination of RSeH to **V-a** leads to the formation of complex **XII**, followed by facile proton transfer by overcoming small activation barriers $\Delta G^{\ddagger}$ = 0.7 and 5.2 kcal/mol for the **XII→XIII-TS** step with sulfur and selenium cores, respectively. Dissociation of RSH from the complex **XIV** furnishes complex **V-b** with a selenium group at the catalyst active site. The reverse process of interconversion of **V-b** to **V-a** is also possible and involves coordination of RSH followed by dissociation of RSeH. Small activation barriers $\Delta G^{\ddagger}$ = 6.2 and 6.7 kcal/mol for the **XIV→XIII-TS** step were calculated with sulfur and selenium cores, respectively. Thus, the exchange of μ_1-coordinated chalcogen groups at the catalyst active site is a feasible process and should proceed fast. According to thermodynamic and kinetic factors formation of complex **XIV** with coordinated selenium group is more favorable.

Considering the overall energetics (Figure 6), the pathway to produce selenium product **XI-b** requires overcoming the **XIV→ VII-b-TS** barrier $\Delta G^{\ddagger}$ = 10.9 and 9.8 kcal/mol for sulfur and selenium cores, respectively. The transformation **XIV→ XI-b** is exothermic with ΔG = −20.7 and −23.6 kcal/mol for sulfur and selenium cores, respectively. The pathway to the sulfur product requires overcoming the higher activation barrier **XIV→VII-a-TS**, where $\Delta G^{\ddagger}$ = 17.8 and 16.6 kcal/mol for sulfur and selenium cores, respectively. The transformation **XIV→ XI-a** is less exothermic with ΔG = −15.3 and −18.0 kcal/mol for sulfur and selenium cores, respectively. Thus, in total agreement with experimental findings RSeH should be involved in the reaction first and should provide vinylic product containing selenium functional group. The relative reactivity of

dx.doi.org/10.1021/ja210596w | *J. Am. Chem. Soc.* 2012, 134, 6637−6649

RSH was found to be significantly lower, and the product with the sulfur group will be formed only after consumption of RSeH.

The above presented mechanistic findings have revealed the Pd−(μ_1-ZR) bond energy as the key factor to determine the reactivity of the catalytic system. To model the three-component PhSeH/PhSH/CySH mixture we have calculated the Pd−(μ_1-ZR) bond energies in the (μ_1-ZR)$Pd_2(SeR)_3$ system (Scheme 7). Amazingly, the calculated Pd−(μ_1-SCy), Pd−(μ_1-SPh), and Pd−(μ_1-SePh) bond energies are in complete agreement with the reaction selectivity ZR = PhSe > PhS > CyS.

Scheme 7. Calculated Thermodynamic Parameters (ΔG, kcal/mol) for Adaptive Recognition of PhSeH, PhSH, and CySH Reagents in the Mixture

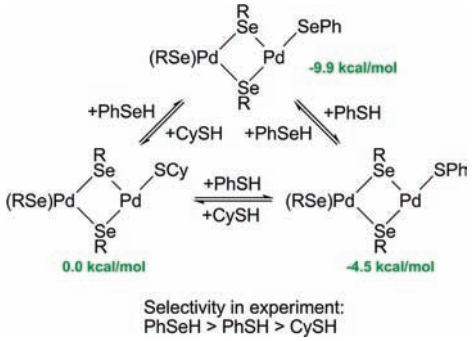

2.9. Extraction of RZH Derivatives from Multicomponent Mixture of Chalcogen Species. Natural sources of sulfur compounds in crude oil represent a heavy mixture, which, in addition to thiols, contains disulfides, cyclic and acyclic sulfides and thiophenes. Our theoretical calculations have shown that substitution of RZ group in the catalyst active center (Scheme 7) by any of the chalcogen derivatives (RSSR, RSR, RSeSeR, C_4H_4S, C_4H_8S) is unlikely, since it is energetically disfavorable by >20 kcal/mol. If this prediction is correct, we should be able to extract thiols directly from such heavy mixtures without a loss of selectivity due to influence of other components.

To verify this prediction we have prepared a mixture of chalcogen compounds containing 10 different derivatives belonging to main classes mentioned above (Scheme 8).

Scheme 8. Extraction of RZH from a Mixture of Chalcogen Species

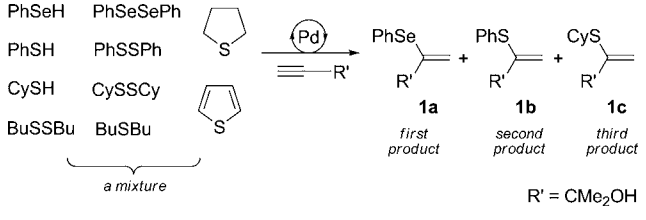

Running the reaction with alkyne using developed catalytic system has shown *complete retain of selectivity*. The product **1a** was formed first in 99% yield, followed by product **1b** in 99% yield and then by product **1c** in 96% yield (Scheme 8). The presence of the other sulfur and selenium compounds in the mixture did not influence activity and selectivity of the catalytic system. High tolerance of the developed catalytic system was in a full agreement with theoretically predicted mechanism and justified potential application for organic synthesis.

3. CONCLUSIONS

The reaction of a simple palladium salt, $Pd(OAc)_2$, with a mixture of SH/SeH compounds produced $Pd(ZR)_2$ species, which under controlled conditions self-assembled to metal−organic structure with outstanding functional properties. Two leading characteristics of the synthesized $[Pd(ZR)_2]_n$ material opened very promising application in catalysis: (i) the $[Pd(ZR)_2]_n$ molecules promote reaction with alkyne and facilitate formation of new carbon-heteroatom bonds (C-Z) in catalytic manner; (ii) binding of ZR groups to the metal center differentiates the reactivity of chalcogens in the Pd−(μ_1-ZR) moiety and induces selectivity in the chemical transformation of interest.

In conclusion, these findings made it possible to develop an efficient and practical procedure for the preparation of sulfur- and selenium-functionalized vinyl compounds starting from alkynes and a mixture of SH/SeH derivatives as initial compounds. The developed approach is of much importance in view of abundant natural sources of sulfur compounds feedstock and easy availability of alkynes.

High efficiency of the developed procedure and excellent dynamic range in toxicity-ordered extraction from the mixture can be of great importance for environmental protection technologies, especially to remove SeH compounds. The extraction procedure captures RSeH compounds into substantially less toxic vinylselenides suitable for practical utilization as reagents in organic synthesis and material science.

The developed system is a rare example of more selective transformation involving heterogeneous catalysts rather than homogeneous catalysts based on similar metal complexes. The mechanism of the catalytic reaction and the origin of high selectivity exhibited in the reaction were established at the molecular level; easy exchange of the ZR groups on the surface of the catalyst (in contrast to the core of the catalyst) and thermodynamic control by Pd−Z bond strength ensure the desired structure of the catalyst active site. It is important to note that catalyst design utilized in the present study does not require any catalyst support; the catalyst was self-organized in situ after the contact with reacting species.

4. EXPERIMENTAL SECTION AND METHODS

4.1. General Experimental Procedures. Unless otherwise noted, the synthetic work was carried out under argon atmosphere. Reagents were obtained from Acros and Aldrich and used as supplied (checked by NMR before use).

All NMR measurements were performed using Bruker DRX-500 and Avance-600 spectrometers operating at 500.1/600.1 and 202.5/243.0 MHz for ^1H and ^{31}P nuclei, respectively. The spectra were processed on a Linux workstation using TopSpin software package. ^1H chemical shifts are reported relative to the corresponding solvent signals used as internal reference, external H_3PO_4/H_2O was used for ^{31}P chemical shifts. Estimated errors in the yields determination by ^1H NMR <2%. The products **1**, **2**, and **3** were identified according to published data.[27] Scanning electron microscopy study was carried out using Hitachi SU-8000 field emission electron microscope, and EDS-SEM analysis was carried out using Hitachi SU-3400 electron microscope.

4.2. Catalytic Addition Reactions in the Three-Component PhSeH/PhSH/CySH Mixture. The alkyne (6.0×10^{-3} mol) was added to $Pd(OAc)_2$ (4.0×10^{-5} mol) and stirred at room temperature until a dark-brown solution was formed (~5 min). PhSeH (2.0×10^{-3} mol), PhSH (2.0×10^{-3} mol), and CySH (2.0×10^{-3} mol) were

dx.doi.org/10.1021/ja210596w | J. Am. Chem. Soc. 2012, 134, 6637−6649

mixed in a separate vessel and were added to the stirred alkyne solution. The stirring was continued for an additional 10 min, and the solution became turbid. The reaction was carried out at 80−120 °C under stirring. Aliquots of the reaction mixture were taken periodically to monitor the reaction by ^{1}H NMR.

4.3. Catalytic Addition Reactions in the Binary Mixtures PhSeH/PhSH, PhSeH/CySH, and PhSH/CySH. The alkyne (4.0×10^{-3} mol) was added to $Pd(OAc)_2$ (4.0×10^{-5} mol) and stirred at room temperature until a dark-brown solution was formed (~5−10 min). PhSeH (2.0×10^{-3} mol) and PhSH (2.0×10^{-3} mol) were mixed in a separate vessel and were added to the stirred alkyne solution. The reaction was carried out at 80−120 °C under stirring. Aliquots of the reaction mixture were taken periodically to monitor the reaction by ^{1}H NMR.

Reactions with PhSeH/CySH and PhSH/CySH binary mixtures were carried out in analogous manner.

4.4. Catalyst Isolation from Reaction Mixture. The alkyne (1.8×10^{-2} mol) was added to $Pd(OAc)_2$ (1.2×10^{-4} mol) and stirred at room temperature until a dark-brown solution was formed (~5 min). PhSeH (6.0×10^{-3} mol), PhSH (6.0×10^{-3} mol), and CySH (6.0×10^{-3} mol) were mixed in a separate vessel and were added to the stirred alkyne solution. The stirring was continued for an additional 10 min, and the solution became turbid. The reaction was carried out at 80 °C under stirring for 25 min to obtain $[Pd(SePh)_2]_n$ particles, 3 h to obtain $[Pd(SePh)_{2-m}(SPh)_m]$ ones. The precipitates were separated by centrifugation (5 min, 5000 rpm), washed with hexanes (4×5 mL), and dried in a vacuum. Dark-brown solids were obtained.

4.5. Preparation of Complex 8. $Pd(OAc)_2$ (0.39 g, 1.34 mmol) and 5 mL of toluene were placed into a 25-mL round-bottom flask equipped with a magnetic stirrer bar. The suspension was stirred at r.t. upon complete dissolution of the palladium acetate. $^nC_6H_{13}SH$ (0.38 mL, 2.67 mmol) was added to the resulting brown solution. The reaction mixture was stirred for 1.5 h at 80 °C. After the reaction was finished, the crude product was purified twice via dry-column, vacuum flash-chromatography (gradient elution with petroleum ether−ethyl-acetate, 4:1 mixture). Purified product was obtained as an orange solid. Yield: 0.32 g, 71%. Crystals suitable for X-ray diffraction experiments were grown from toluene−petroleum ether, 1:1 mixture, at room temperature.

^{1}H NMR (500.1 MHz; CDCl3; δ, ppm; J, Hz): 3.03−3.11 (t, 2H), 2.80−2.89 (t, 2H), 2.10−2.24 (m, 2H), 2.00−2.10 (m, 2H), 1.67−1.78 (m, 2H), 1.55−1.65 (m, 2H), 1.31−1.54 (m, 8H), 0.91−1.09 (m, 6H). ^{13}C{^{1}H} NMR (125.8 MHz; $CDCl_3$; δ, ppm): 35.53, 35.37, 33.55, 32.38, 31.87, 31.28, 29.22, 29.01, 23.09, 14.35, 14.32. HRMS(ESI): Calculated for $C_{72}H_{156}Pd_6S_{12}$ [M + nH] = 2045.3185, found 2045.3180 (Δ = 1.2 ppm). Elemental analysis: Calculated for $C_{72}H_{156}Pd_6S_{12}$ (%): C, 42.48; H, 7.69; Pd, 31.22; S, 18.81; found: C, 42.56; H, 7.65; Pd, 31.12; S, 18.91.

4.6. Dynamically Changed Mixture of Reagents and Dynamic Range Test. The alkyne (2.0×10^{-3} mol) was added to $Pd(OAc)_2$ (2.0×10^{-5} mol) and stirred at room temperature until a dark-brown solution was formed (~5−10 min). PhSH (1.0×10^{-3} mol) and CySH (1.0×10^{-3} mol) were mixed in a separate vessel and were added to the stirred alkyne solution. The stirring was continued for additional 10 min, and a dark-brown suspension was formed. The reaction was carried out for 2 h at 80 °C under stirring. Aliquots of the reaction mixture were taken periodically to monitor the reaction by ^{1}H NMR. After 2 h PhSeH (1.0×10^{-3} mol) was added to the reaction mixture. The reaction was continued for an additional 10 h at 80−120 °C under stirring. Aliquots of the reaction mixture were taken periodically to monitor the reaction by ^{1}H NMR.

4.7. Catalytic Reaction in Multicomponent Mixture. The alkyne (6.0×10^{-3} mol) was added to $Pd(OAc)_2$ (4.0×10^{-5} mol) and stirred at room temperature until a dark-brown solution was formed (~5 min). Ph_2Se_2 (5.0×10^{-4} mol), Ph_2S_2 (5.0×10^{-4} mol), Cy_2S_2 (5.0×10^{-4} mol), Bu_2S_2 (5.0×10^{-4} mol), Bu_2S (5.0×10^{-4} mol), thiophene (5.0×10^{-4} mol), and tetrahydrothiophene (5.0×10^{-4} mol) were mixed in a separate vessel, and the 0.34 mL aliquote of PhSeH (1.0×10^{-3} mol), PhSH (1.0×10^{-3} mol) and CySH (1.0×10^{-3} mol) was added to the mixture. The resulted mixture was added to the stirred alkyne solution at ~5 °C (water/ice bath). The stirring was continued for an additional 10 min, and the solution became turbid. The reaction was carried out at 80−120 °C under stirring. Aliquots of the reaction mixture were taken periodically to monitor the reaction by ^{1}H NMR.

4.7. X-ray Structural Study of Complex 8. Data were collected on a Bruker three-circle diffractometer equipped with a SMART 1K CCD detector and corrected for absorption using the *SADABS* program.[28] Data reduction was performed using *SMART2* and *SAINTPlus3* programs. The structure was solved by direct methods and refined by full-matrix least-squares technique on F^2 with anisotropic displacement parameters for all the non-H atoms (for details, see Supporting Information). The H atoms were placed in calculated positions and refined within the riding model with fixed isotropic displacement parameters (Uiso(H) = 1.5 Ueq(C) for the CH_3 groups and Uiso(H) = 1.2 Ueq(C) for the other groups). All calculations were carried out using the *SHELXTL* program.[29] Crystallographic data for the structure reported in this study have been deposited with the Cambridge Crystallographic Data Centre as supplementary CCDC.

4.8. Theoretical Calculations. Geometry and energy of the reactants, intermediates, transition states, and products of the reactions were calculated using the B3LYP hybrid density functional method[30] in conjunction with standard 6-31G(d) basis set[31] for H, C, O, S, and Se and Lanl2dz basis set with effective core potentials[32] for the metal (denoted as B3LYP/6-31G(d) and Lanl2dz level). In previous studies it was established that this level of theory reasonably describes the energy and geometry parameters of the systems involving transition metal complexes.[33]

For all studied structures normal coordinate analysis was performed to characterize the nature of the stationary points and to calculate thermodynamic properties (298.15 K and 1 atm). Transition states were confirmed with IRC (Intrinsic Reaction Coordinate) calculations using the standard method.[34] All calculations were performed without any symmetry constraints using the *Gaussian09* program.[35]

■ ASSOCIATED CONTENT

Supporting Information

^{1}H and ^{13}C NMR spectra of complex **8**, line assignment of complex **8** with TOCSY and HSQC NMR, X-ray structure analysis and details on theoretical study. This material is available free of charge via the Internet at http://pubs.acs.org.

■ AUTHOR INFORMATION

Corresponding Author

(V.P.A.) val@ioc.ac.ru; (D.G.M.) dmusaev@emory.edu

Notes

The authors declare no competing financial interest.

■ ACKNOWLEDGMENTS

V.P.A. acknowledges the Emerson Center Fellowship. The work was supported in part by the Russian Foundation for Basic Research (Project No. 10-03-00370), Grant MD-4969.2012.3 and Programs of Division of Chemistry and Material Sciences of RAS. We gratefully acknowledge NSF MRI-R2 Grant (CHE-0958205) and the use of the resources of the Cherry Emerson Center for Scientific Computation. D.G.M gratefully acknowledge the NSF Center of Chemical Innovation in Stereoselective C¬H Functionalization (CHE-0943980) for support.

■ REFERENCES

(1) Topsøe, H., Clausen, B. S., Massoth, F. E. *Hydrotreating Catalysis*; Springer-Verlag: New York, 1996.

(2) Kabe, T., Ishihara, A., Qian, W. *Hydrodesulfurization and Hydrodenitrogenation*; Wiley-VCH: New York, 1999.

(3) Song, C. *Catal. Today* **2003**, *86*, 211.
(4) Babich, I. V.; Moulijn, J. A. *Fuel* **2003**, *82*, 607.
(5) *Sulfur Production Report*, U.S. Geological Survey, January 2011; http://minerals.usgs.gov/minerals/pubs/commodity/sulfur/mcs-2011-sulfu.pdf.
(6) Metal-catalyzed Z−H additions: (a) Beletskaya, I. P.; Ananikov, V. P. *Chem. Rev.* **2011**, *111*, 1596. (b) Bichler, P.; Love, J. A. *Top. Organomet. Chem.* **2010**, *31*, 39. (c) Weiss, C. J.; Marks, T. J. *Dalton Trans.* **2010**, *39*, 6576. (d) Ogawa, A. *J. Organomet. Chem.* **2000**, *611*, 463. (e) Kuniyasu, H.; Ogawa, A.; Sato, K.; Ryu, I.; Kambe, N.; Sonoda, N. *J. Am. Chem. Soc.* **1992**, *114*, 5902. (f) Ishii, A.; Kamon, H.; Murakami, K.; Nakata, N. *Eur. J. Org. Chem.* **2010**, 1653. (g) Ishii, A.; Nakata, N.; Uchiumi, R.; Murakami, K. *Angew. Chem., Int. Ed.* **2008**, *47*, 2661. (h) Nakata, N.; Yamaguchi, Y.; Ishii, A. *J. Organomet. Chem.* **2010**, *695*, 970.
(7) Sheldon, R. A. *Pure Appl. Chem.* **2000**, *72*, 1233.
(8) Anastas, P. T.; Warner, J. C. *Green Chemistry; Theory and Practice*; Oxford University Press: New York, 1998.
(9) (a) Baeckvall, J.-E.; Ericsson, A. *J. Org. Chem.* **1994**, *59*, 5850. (b) Kuniyasu, H.; Ogawa, A.; Sato, K.-I.; Ryu, I.; Sonoda, N. *Tetrahedron Lett.* **1992**, *38*, 5525. (c) Kamiya, I.; Nishinaka, E.; Ogawa, A. *J. Org. Chem.* **2005**, *70*, 696.
(10) Akelah, A.; Moet, A. *Functionalized Polymers and Their Applications*; Chapman and Hall: New York, 1990.
(11) Paquette, L. A., Ed. In *Sulfur-Containing Reagents*; Wiley-Blackwell: New York, 2010.
(12) McReynolds, M. D.; Dougherty, J. M.; Hanson, P. R. *Chem. Rev.* **2004**, *104*, 2239.
(13) Patai, S.; Rappoport, Z., Eds. In *The Chemistry of Organic Selenium and Tellurium Compounds*; John Wiley and Sons: New York, 1986−1987; Vols. *1*−*2*.
(14) (a) Ananikov, V. P.; Beletskaya, I. P. *Dalton Trans.* **2011**, *40*, 4011. (b) Ananikov, V. P.; Orlov, N. V.; Beletskaya, I. P.; Khrustalev, V. N.; Antipin, M. Yu.; Timofeeva, T. V. *J. Am. Chem. Soc.* **2007**, *129*, 7252.
(15) Ananikov, V. P.; Malyshev, D. A.; Beletskaya, D. A.; Aleksandrov, G. G.; Eremenko, I. L. *J. Organomet. Chem.* **2003**, *679*, 162.
(16) Ananikov, V. P.; Malyshev, D. A.; Beletskaya, I. P.; Aleksandrov, G. G.; Eremenko, I. L. *Adv. Synth. Catal.* **2005**, *347*, 1993.
(17) Jin, Z.; Xu, B.; Hammond, G. B. *Eur. J. Org. Chem.* **2010**, 168.
(18) Trofimov, B. A. *Curr. Org. Chem.* **2002**, *6*, 1121.
(19) Perin, G.; Lenardão, E. J.; Jacob, R. G.; Panatieri, R. B. *Chem. Rev.* **2009**, *109*, 1277.
(20) The concentration of phosphine ligands was adjusted to stabilize the complexes in solution, and ^{31}P NMR chemical shifts of the complexes (δ = 98.8 ppm, 101.2 ppm) were identified according to NMR analysis described earlier: Ananikov, V. P.; Zalesskiy, S. S.; Kachala, V. V.; Beletskaya, I. P. *J. Organomet. Chem.* **2011**, *696*, 400.
(21) Phosphine or other strong ligands occupy vacancies in the coordination sphere of the metal and prevent formation of polymeric metal species.
(22) Complete set of calculations for n = 2, 3, 4, 5, 6, 7, 8, and 9 (chain structures) and n = 3, 4, 5, 6, 7, 8, and 9 (cyclic structures) with both Z = S and Se were carried out; see Supporting Information for details.
(23) Calculated energy surface of mononuclear complexes **I**−**IV** is shown in Scheme S2 for comparison (see Supporting Information); this pathway is not discussed in details here.
(24) Coordination of alkyne to the metal center was calculated to be exothermic by −1 to −3 kcal/mol on the ΔG surface and by −11 to −14 kcal/mol on the ΔE and ΔH surfaces. Thus, it can be considered as a weakly bound π-complex on the ΔG surface. See Table S11 in the Supporting Information for details.
(25) Note also, that reductive elimination involving chelate ligand was not observed: Ananikov, V. P.; Mitchenko, S. A.; Beletskaya, I. P. *J. Organomet. Chem.* **2000**, *604*, 290.
(26) (a) Spek, A. L. *Cambridge Crystallographic Database*; refcode AFACUG, 2007. (b) Stash, A. I.; Perepelkova, T. I.; Noskov, Yu. G.; Buslaeva, T. M.; Romm, I. P. *Russ. J. Coord. Chem.* **2001**, *27*, 585. (c) Yang, Z.; Smetana, A. B.; Sorensen, C. M.; Klabunde, K. J. *Inorg. Chem.* **2007**, *46*, 2427. (d) Schneider, I.; Horner, M.; Olendzki, R. N.; Strahle, J. *Acta Crystallogr.* **1993**, *C49*, 2091.
(27) (a) Ananikov, V. P.; Orlov, N. V.; Beletskaya, I. P. *Organometallics* **2006**, *25*, 1970. (b) Ananikov, V. P.; Orlov, N. V.; Beletskaya, I. P. *Organometallics* **2007**, *26*, 740.
(28) Sheldrick, G. M. *SADABS*; Bruker AXS Inc.: Madison, WI, 1997.
(29) Sheldrick, G. M. *SHELXTL-97*, Version 5.10; Bruker AXS Inc.: Madison, WI, 1997.
(30) (a) Becke, A. D. *Phys. Rev. A* **1988**, *38*, 3098. (b) Lee, C.; Yang, W.; Parr, R. G. *Phys. Rev. B* **1988**, *37*, 785. (c) Becke, A. D. *J. Chem. Phys.* **1993**, *98*, 5648.
(31) (a) Ditchfield, R.; Hehre, W. J.; Pople, J. A. *J. Chem. Phys.* **1971**, *54*, 724. (b) Hehre, W. J.; Ditchfield, R.; Pople, J. A. *J. Chem. Phys.* **1972**, *56*, 2257.
(32) (a) Hay, P. J.; Wadt, W. R. *J. Chem. Phys.* **1985**, *82*, 270. (b) Wadt, W. R.; Hay, P. J. *J. Chem. Phys.* **1985**, *82*, 284. (c) Hay, P. J.; Wadt, W. R. *J. Chem. Phys.* **1985**, *82*, 299. (d) Dunning, T. H., Jr.; Hay, P. J. In *Modern Theoretical Chemistry*; Schaefer, H. F., III, Ed.; Plenum: New York, 1976; Vol. *3*, pp 1−28.
(33) (a) Cramer, C. J.; Truhlar, D. G. *Phys. Chem. Chem. Phys.* **2009**, *11*, 10757. (b) Ananikov, V. P.; Musaev, D. G.; Morokuma, K. *J. Mol. Catal. A: Chem.* **2010**, *324*, 104.
(34) (a) Gonzalez, C.; Schlegel, H. B. *J. Chem. Phys.* **1989**, *90*, 2154. (b) Gonzalez, C.; Schlegel, H. B. *J. Phys. Chem.* **1990**, *94*, 5523.
(35) Frisch, M. J. ;et al.et al. *Gaussian 09*; Gaussian, Inc.: Pittsburgh PA, 2009.